tvst

DOI: 10.1167/tvst.4.2.13

Article

Effects of Detergent-Based Protocols on Decellularization of Corneas With Sclerocorneal Limbus. Evaluation of Regional Differences

Miguel González-Andrades[1,2], Victor Carriel[1], Mario Rivera-Izquierdo[1], Ingrid Garzón[1], Elena González-Andrades[1], Santiago Medialdea[3], Miguel Alaminos[1], and Antonio Campos[1]

[1] Tissue Engineering Group, Department of Histology, University of Granada, Spain and Instituto de Investigación Biosanitaria ibs.GRANADA, Spain

[2] Division of Ophthalmology, University Hospital San Cecilio, Granada, Spain

[3] Division of Ophthalmology, University Hospital Virgen de las Nieves, Granada, Spain

Correspondence: Antonio Campos, Department of Histology, Faculty of Medicine, University of Granada, Avenida de Madrid 11, E18012, Granada, Spain; e-mail: acampos@ugr.es

Received: 4 September 2014
Accepted: 21 January 2015
Published: 17 April 2015

Keywords: cornea regions; decellularization protocols; tissue engineering; sclerocorneal limbus; extracellular matrix

Citation: González-Andrades M, Carriel V, Rivera-Izquierdo M, et al. Effects of detergent-based protocols on decelluarization of corneas with sclerocorneal limbus. Evaluation of regional differences. Tran Vis Sci Tech. 2014;4(2):13, http://tvstjournal.org/doi/full/10.1167/tvst.4.2.13, doi: 10.1167/tvst.4.2.13

Purpose: In this work, we decellularized whole porcine corneas including the sclerocorneal limbus (SCL) and we evaluated regional differences in order to identify an efficient method to decellularize whole corneas for future clinical use.

Methods: We analyzed the efficiency of four decellularization protocols based on benzalkonium chloride (BAK), Igepal, sodium dodecyl sulfate (SDS), and Triton X-100 detergents on whole porcine corneas.

Results: Results showed that the decellularization efficiency of most protocols was low, with the specific protocol resulting in more efficient levels of decellularization being 0.1% SDS for 48 hours, especially in the medium and posterior cornea regions. A significant correlation was found between the decellularization efficiency and the concentration of agent used ($P = 0.0174$; $r = 0.1540$), but not for the incubation time ($P > 0.05$). The analysis of cornea components preservation demonstrated that all protocols were able to preserve the integrity of the Bowman's layer and Descemet's membrane. Although the collagen structure was partially altered, the global decellularization groups showing highest preservation of the ECM collagen contents and orientation were Igepal and SDS, with differences among the three regions of the cornea. All global groups showed high levels of proteoglycan and glycoprotein preservation after decellularization, with the best results were found in the SDS group followed by the Igepal group.

Conclusions: These results suggest that very powerful protocols are necessary for whole-cornea decellularization. For the generation of lamelar corneas for clinical use, decellularization regional differences should be taken into account.

Translational Relevance: Decellularized whole corneas may be potential therapeutic agents for lamelar keratoplasty.

Introduction

Corneal diseases are the second cause of blindness worldwide and the responsible of 90% of cases of blindness in some regions of Africa.[1] Moreover, corneal trauma and ulcers are associated to nearly 2 million of monocular blind patients every year.[2] In most cases, allogeneic corneal transplant is the only successful treatment for corneal blindness. However, there is a chronic shortage of human donor corneas, especially in developing countries,[3] and novel therapeutic alternatives are in need.

Tissue engineering appears as a promising discipline whose aim is to generate artificial tissues and organs that can replace damaged tissues in the human body, including the cornea.[4,5] Different biomaterials have been proposed as cornea matrix substitutes, including fibrin,[6] fibrin-agarose,[7] collagen,[8] silk,[9] and

decellularized porcine corneas.[10] In this regard, acellular corneas based on decellularization protocols applied to animal or nonviable human corneas could represent a real alternative to fresh human donor corneas. Several methods have been published to the date, but none of them have been established as a reliable or standardized protocol for cornea decellularization, especially in the case of the human cornea, and published decellularization protocols often lack full characterization of the decellularized tissues.[11] In a previous work, we demonstrated the efficacy of sodium dodecyl sulfate (SDS) and sodium chloride (NaCl) to decellularize porcine corneal stromas after using dispase II.[10] Afterwards, Shafiq et al.[12] modified our method based on NaCl by adding nucleases to the protocol, and they demonstrated that this protocol could be associated to undetectable levels of cellular material in human corneas, supporting both fibroblast and epithelial cell growth in vitro. On the other hand, we recently demonstrated that the use of decellularized extracellular matrix (ECM) obtained from extraocular tissues, such as the small intestine could permit generating bioengineered cornea substitutes with potential clinical usefulness and translational perspectives.[13]

Among all available decellularization methods, those based on the use of detergents are likely the most simple and inexpensive, although none of these methods have been tried for decellularization of whole corneas including the sclerocorneal limbus (SCL), which is essential for cornea cell physiology and regeneration. This could be of interest if limbal stem cells are used in the future to repopulate the SCL of decellularized corneas. Although decellularized corneas may provide a scaffold able to support corneal cells growth, simpler and cheaper protocols should be developed, especially for whole-corneas decellularization. These protocols should be able to remove all cells from the animal cornea, while maintaining all major ECM components of the tissue. Furthermore, the effects of each decellularization agent on the different regions of the cornea have not been fully elucidated, and most reports analyzed the decellularization process globally. This is especially important for a more appropriate selection of the cornea regions that could be used clinically for lamelar keratoplasty.

In the present study, several detergent-based enzyme-free decellularization protocols were evaluated on whole-porcine corneas including the SCL at different concentrations and times to determine their effects on the different regions of the cornea. These decellularized corneas may have future translational potential for the treatment of corneal diseases.

Materials and Methods

Decellularization of Porcine Corneas

Fresh porcine eyes were obtained from adult pigs immediately after their death at a local slaughterhouse. The eyes selected for the study had integral corneal surface with a horizontal corneal diameter of 12 to 14 mm. The native porcine cornea (NPC) with 1-mm scleral ring was removed using Wescott scissors. Corneas were washed thoroughly with 10% antibiotic–antimycotic solution (Invitrogen-Gibco, Carlsbad, CA) in phosphate-buffered saline (PBS) for 10 minutes and then washed in PBS. Several independent decellularization protocols based on benzalkonium chloride (BAK), Igepal, SDS, or Triton X-100 (all of them from Sigma-Aldrich, Steinheim, Germany) were applied to the NPCs at different concentrations (0.01%, 0.05%, and 0.1%) and times (12, 24, and 48 hours) for each of the agents used, except for control NPCs that remained as native nondecellularized corneas. Afterwards, porcine corneas were washed with PBS for 24 hours. All solutions in which porcine corneas were immersed had a mass ratio of 20:1 (solution:cornea), and all protocols were carried out with continuous shaking (300 rpm) at room temperature. Every 12 hours, all decellularization media were renewed. Decellularized porcine corneas (DPC) were then placed between two pieces of absorbent paper and incubated in a dry chamber at 60°C for 1 hour to eliminate the excess liquid. In total, 33 different study groups were established, and three samples were analyzed per condition: native nondecellularized corneas; corneas decellularized with BAK at three concentrations (0.01%, 0.05%, and 0.1%) for three different times (12, 24, and 48 hours); corneas decellularized with Igepal at three concentrations (0.01%, 0.05%, and 0.1%) for three different times (12, 24, and 48 hours); corneas decellularized with SDS at three concentrations (0.01%, 0.05%, and 0.1%) for three different times (12, 24, and 48 hours); corneas decellularized with Triton X-100 at three concentrations (0.01%, 0.05%, and 0.1%) for three different times (12, 24, and 48 hours).

All experimental protocols, including the use of animal tissues, were approved by the institutional local ethics and research committee. This work adhered to the Declaration of Helsinki.

Histology Evaluation and Image Processing Analysis

For light microscopy, NPC and DPC were fixed in 4% formaldehyde, dehydrated in increasing concentrations of ethanol (70°, 96°, 100°) for 30 minutes each one, immersed twice in xylene for 30 minutes each time, and in liquid paraffin for 30 minutes each time for impregnation. Tissue sections 5-μm thick were obtained with a microtome. To determine the effectiveness of cell removal (decellularization efficiency), the number of remaining nuclei in control and decellularized corneas was quantified by using 4,6-diamidino-2-phenylindole (DAPI) staining (Sigma-Aldrich) on deparaffinized tissue sections,[13] and the percentage of cell removal was determined for DPC samples. The number of remaining nuclear debris was determined per field. Before analyzing the number of particles in a 16-bits image that was autothreshold (moments mode used), we previously subtracted the background (50 pixels) and sharpened the image. The percentage of cells or cell fragments removed was calculated by using the number of remaining cells or cell fragments present in the controls as a reference.

For quantitative analysis of the ECM, histochemistry was carried out to detect the main fibrillar and nonfibrillar ECM components on tissue sections as previously described by Oliveira et al.[13] (all reagents were purchased to Sigma-Aldrich):

1. To evaluate the presence of collagen fibers, picrosirius red staining was performed using Sirius red F3B working solution for 30 minutes and Harris's hematoxylin counterstaining for 5 minutes. These samples were analyzed by using light and polarized light microscopy;
2. To assess glycoproteins content, the Periodic acid-Schiff staining method (PAS) was used with 0.5% periodic acid solution was used for 5 minutes as oxidant, followed by incubation in Schiff reagent for 15 minutes, and counterstaining with Harris's hematoxylin for 1 minute; and
3. To determine proteoglycans content, samples were incubated in alcian blue solution for 30 minutes and counterstained with nuclear fast red solution for 1 minute.

In all cases, DAPI staining and histochemistry were carried out at the same time for all samples, using the same reagents and the same times to ensure reproducibility of the results. Histological images were taken using a light microscope (Eclipse i90; Nikon, Tokyo, Japan) using exactly the same conditions (exposition time, white balance, background, etc.) with the Nikon NIS-Elements software. Subsequently, samples were quantitatively analyzed by using the image processing software ImageJ 1.43 m (National Institutes of Health, Bethesda, MD). Three different corneal stroma regions of each sample were independently analyzed, corresponding to the anterior region, the middle region and the posterior region of the cornea. The size of the area analyzed for each region was 0.07 mm^2, and three areas were analyzed per region.

The intensity of the staining of each specific ECM component was quantified by using ImageJ software (32-bit images were analyzed using plot profiles). The data obtained were normalized using plot profiles from white images of the regions in the sample where DPC were not present, comparing the samples with the control, which was established as the maximum value to obtain percentages of staining intensity per each kind of stain used.

Surface characterization and analysis of stromal fiber orientation of the samples stained with picrosirius red was performed with SurfCharJ ImageJ plug-in for surface assessment. This plug-in allows for the calculation of structure orientation based on the mean resultant vector (MRV) and plots the frequency of azimuthal angles for estimating the preferred orientation. To analyze the fiber orientation of the whole DPC, we first obtained individual pictures of the anterior, medial, and posterior region of the cornea. Then, the analysis was carried out individually for each picture, and average values were calculated for the MRV.

Statistical Analysis

First, we determined the average and standard deviation of each of the following experimental groups: (1) all samples treated with SDS, Triton X-100, Igepal, or BAK independently of the concentration and time used (for instance, all samples treated with SDS regardless the specific conditions). These groups were named as global groups, and (2) samples treated with a specific concentration and time of each agent (for instance, samples treated with 0.1% SDS for 12 hours). These groups were named as specific groups.

Then, to compare the results obtained among different groups, the Kruskal-Wallis test was used. In cases with significant differences among groups as determined by this test, Mann-Whitney *U* test was used to identify statistical differences between

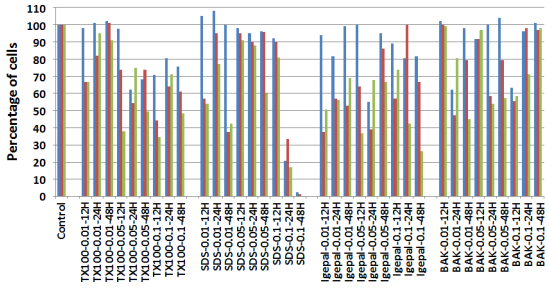

Figure 1. Decellularization efficiency based on histological analysis using DAPI staining of NPC and DPC subjected to the different decellularization protocols. The percentage of remaining cells or cell debris is shown for each group of samples and for the anterior (*blue*), medium (*red*), and posterior (*green*) areas of the cornea ($n = 3$) using NPC as control. TX100: Triton X-100.

two different groups, for example, NPC versus specific DPC groups. To determine the correlation between the type of decellularization agent used and the presence of a specific tissue component, we used the Kendall tau correlation test. All tests were performed two-tailed and a Bonferroni-adjusted P value below 0.001 was considered as statistically significant since up to 30 statistical tests were carried out.

Results

Decellularization Efficiency

Our analysis first showed that keratocytes tended to localize preferentially in specific areas of the stroma of the native control NPC, with a high number of cells allocated in the anterior region and very few cells in the posterior region of the stroma. Then, the histological analysis using DAPI staining of DPC subjected to the different decellularization protocols revealed a great variability among the different protocols. Although most conditions were able to eliminate a significant percentage of cells from the corneas, very few protocols succeeded in eliminating more than 90% of the tissue cells (Fig. 1 and Table 1). However, some specific times and concentrations resulted in more efficient levels of decellularization than others ($P < 0.001$ for the comparison among all global groups using the Kruskal-Wallis test). The most efficient protocol was based on the use of 0.1% SDS for 48 hours, which led to a complete cell elimination from the posterior region of the cornea (0% remaining cells; $P < 0.001$ as compared with control corneas for the Mann-Whitney U test), although few minuscule nuclear debris remained in the anterior (2.4%; $P < 0.001$) and medium fields (1.4%; $P < 0.001$). The correlation between the decellularization efficiency and the concentration of agent did not reach statistical significance ($P = 0.0174$; $r = 0.1540$), and correlation with the incubation time was very low ($P > 0.05$).

Preservation of Tissue Structure and Composition After Cornea Decellularization

The analysis of decellularized DPC demonstrated that all decellularization protocols were able to preserve the integrity of the Bowman's layer and Descemet's membrane (Fig. 2).

Detection of collagen fibers in control native NPC showed a well-defined pattern in which an anterior, a medium, and a posterior stroma region were identifiable. First, the anterior region, corresponding to approximately 20% to 30% of the stroma thickness, was characterized by the presence of collagen lamellae with less compactation than lamellae corresponding to the other regions. Then, the medium region of the stroma accounted for 50% to 60% of the thickness and showed highly compacted collagen lamellae, whereas the posterior region corresponded to approximately 10% to 15% of the cornea thickness and had highly compacted collagen lamellae showing less staining intensity than the medium region (Fig. 2).

The analysis of collagen preservation in decellularized corneas demonstrated that all global and specific decellularization methods resulted in certain degrees of collagen intensity loss, with significant differences among all global study groups ($P < 0.001$ for the Kruskal-Wallis test). The global decellularization groups showing highest preservation of the ECM collagen content were Igepal and SDS, although all groups were statistically different to control undecellularized corneas ($P > 0.05$ for the Mann-Whitney U test; Fig. 3 and Table 1). The analysis of the different regions of the decellularized cornea showed that the anterior cornea preserved higher amounts of collagen fibers than the rest of the organ. A significant correlation was found between the collagen content and the type of decellularization agent ($P < 0.001$; $r = 0.0643$), the concentration ($P < 0.001$; $r = 0.0776$), and the region of the cornea ($P < 0.001$; $r = 0.0243$), but not for the decellularization time ($P > 0.05$). Fiber orientation analysis using the SurfCharJ ImageJ plug-in demonstrated that corneas subjected to

decellularization showed an orientated fiber distribution that was very similar to control NPCs, except for corneas decellularized with BAK, which showed a significant alteration of the fibrillar pattern ($P < 0.001$ as compared with NPCs). Although no statistically significant differences were found between control corneas and corneas decellularized with Triton X-100, Igepal, and SDS, the agent that showed more proper fiber alignment was SDS (Fig. 4 and Table 1).

For proteoglycan detection, control, and decellularized corneas were stained with alcian blue. In this regard, both the anterior and the posterior regions of the stroma of the NPC were characterized by a high concentration of proteoglycans, whereas the medium region had very few amounts of these components. The analysis of decellularized corneas using alcian blue staining revealed that most protocols were able to maintain the proteoglycan contents of the porcine cornea, although some differences existed among protocols ($P < 0.001$ for the Kruskal-Wallis test). All global groups showed high levels of proteoglycan preservation after decellularization, similar to the control corneas, and the most proper results were found in the SDS group followed by the Igepal group (differences were nonsignificant among groups). Strikingly, the anterior region of the cornea showed significant loss of proteoglycans after decellularization (Fig. 5 and Table 2), whereas no differences with the control corneas were found for the medium and posterior cornea regions or for the full-thickness cornea. The statistical analysis showed a significant correlation between the amount of proteoglycans preserved in the decellularized cornea and the type of decellularization agent ($P < 0.001$; $r = 0.1956$), the concentration ($P < 0.001$; $r = 0.1882$), time ($P < 0.001$; $r = 0.1642$), and the region of the cornea ($P < 0.001$; $r = 0.1999$).

Quantification of glycoproteins using PAS analysis in control NPC demonstrated that these components were very abundant in the medium region of the stroma, with lower concentrations in the anterior and posterior regions. The analysis of decellularized corneas showed that the decellularization process significantly altered the amount of these components in the cornea ECM, with significant differences among groups ($P < 0.001$ for the Kruskal-Wallis test). All global groups were statistically different to the controls ($P < 0.001$ for the Mann-Whitney U test). The global groups that more efficiently preserved the glycoprotein contents of the ECM were SDS (78.3 ± 39.8 for the full-thickness cornea) followed by Igepal (66.4 ± 6.4). Both were significantly better ($P < 0.001$ for the Mann-Whitney U test) than corneas decellularized with Triton X-100 (54.7 ± 8.1) or BAK (60.6 ± 13.6). In this case, the anterior region of the cornea showed the highest concentrations of glycoproteins after decellularization (Fig. 6 and Table 2). A significant correlation was found between the remaining percentage of glycoproteins and the decellularization time ($P < 0.001$, $r = 0.2329$), the concentration of decellularization agent ($P < 0.001$, $r = 0.1497$), and the cornea region ($P < 0.001$; $r = 0.2333$).

Discussion

Different decellularization agents have been used for cornea decellularization, although no consensus protocols have been described.[11,14] In addition, most published protocols used only the central corneal button, and no experience is available on decellularization of the whole cornea, including the SCL. Decellularization of animal corneas including the SCL could be useful for the generation of complete bioengineered corneas including the area where cornea stem cells reside, and it opens the door to the possibility of generating whole-cornea substitutes for clinical use. From a translational standpoint, these substitutes could have clinical potential as substitutes of the whole cornea with SCL once recellularized. One of the main problems associated to cornea decellularization is the need of eliminating all cells and nuclear fragments from the native cornea.[10,15,16] In cases when the SCL is present, this structure may act as a physical barrier preventing the efficient outflow of cells and cell debris. Therefore, novel specific decellularization methods should be developed for decellularization of whole corneas and their effects on the different regions of the cornea should be determined.

In this work, we have used different previously described decellularization detergents for whole-cornea decellularization. These agents were selected due to their decellularization power and in agreement with previous reports describing the use of detergents for decellularization of animal corneas or other organs. SDS and Triton X-100 have been widely applied to decellularize corneas,[12,17–21] and Igepal and BAK were selected for the first time to determine their usefulness for cornea decellularization. Igepal has been previously used for decellularizing heart valves,[22] pericardium,[23] or veins.[24] BAK

Table 1. Quantitative Analysis of Decellularization Efficiency as Determined by DAPI Staining, Collagen Preservation as Determined by Picrosirius Red Histochemical Staining and Collagen Fibers Orientation Based on the Evaluation of MRV Using the SurfCharJ ImageJ Software

	DAPI Ant	DAPI Med	DAPI Post	Normalized DAPI Ant	Normalized DAPI Med	Normalized DAPI Post	Picrosirius Ant
Control NPC	41	36	43.5	100	100	100	154.4
TX100-0.01, 12 h	40.2	24	29	98	66.7	66.7	70.5
TX100-0.01, 24 h	41.4	29.5	41.3	101	81.9	95	74.0
TX100-0.01, 48 h	41.8	36.4	39.5	102	101	90.8	68.8
TX100-0.05, 12 h	40	26.5	16.5	97.6	73.6	37.9	128.1
TX100-0.05, 24 h	25.5	19.5	32.5	62.2	54.2	74.7	109.2
TX100-0.05, 48 h	28	26.5	21.5	68.3	73.6	49.4	107.9
TX100-0.1, 12 h	29	16	15	70.7	44.4	34.5	98.7
TX100-0.1, 24 h	33	23	31	80.5	63.9	71.3	123.3
TX100-0.1, 48 h	31	22	21	75.6	61.1	48.3	131.4
SDS-0.01, 12 h	43.1	20.5	23.5	105	56.9	54	159.3
SDS-0.01, 24 h	44.3	34.2	33.5	108	95	77	120.3
SDS-0.01, 48 h	41	13.5	18.5	100	37.5	42.5	134.7
SDS-0.05, 12 h	40.2	34.2	39.6	98	95	91	78.4
SDS-0.05, 24 h	39	32.4	38.3	95	90	88	65.2
SDS-0.05, 48 h	39.4	34.5	26	96.1	95.8	59.8	66.6
SDS-0.1, 12 h	37.7	32.4	35.2	92	90	81	92.4
SDS-0.1, 24 h	8.5	12	7.5	20.7	33.3	17.2	81.2
SDS-0.1, 48 h	1	0.5	0	2.4	1.4	0	82.3
Igepal-0.01, 12 h	38.5	13.5	22	94	37.5	50.6	94.0
Igepal-0.01, 24 h	33.5	20.5	24.5	81.7	56.9	56.3	125.1
Igepal-0.01, 48 h	40.6	19	30	99	52.8	69	129.0
Igepal-0.05, 12 h	41	23	16	100	63.9	36.8	73.1
Igepal-0.05, 24 h	22.5	14	29.5	54.9	38.9	67.8	91.4
Igepal-0.05, 48 h	39	31	29	95.1	86.1	66.7	57.3
Igepal-0.1, 12 h	36.5	20.5	32	89	56.9	73.6	116.2
Igepal-0.1, 24 h	33	36	18.5	80.5	100	42.5	141.8
Igepal-0.1, 48 h	33.5	24	11.5	81.7	66.7	26.4	146.6
BAK-0.01, 12 h	41.8	36	43.1	102	100	99.1	73.1
BAK-0.01, 24 h	25.5	17	35	62.2	47.2	80.5	58.7
BAK-0.01, 48 h	40.2	28.5	19.5	98	79.2	44.8	41.3
BAK-0.05, 12 h	37.5	33	42.2	91.5	91.7	97	66.1
BAK-0.05, 24 h	41	21	23.5	100	58.3	54	57.5
BAK-0.05, 48 h	42.6	28.5	25	104	79.2	57.5	62.4
BAK-0.1, 12 h	26	20	25.5	63.4	55.6	58.6	105.3
BAK-0.1, 24 h	39.4	35.3	31	96.1	98.1	71.3	83.3
BAK-0.1, 48 h	41.4	34.9	42.6	101	96.9	97.9	68.7

For DAPI and picrosirius, average results are shown for each sample as raw values and normalized values after considering the results obtained for control NPC as 100%. Control NPC: native undecellularized corneas. Notes: Ant: anterior area of the cornea; Med: medium area of the cornea; Post: posterior area of the cornea.

Table 1. Extended.

Picrosirius Med	Picrosirius Post	Normalized Picrosirius Ant	Normalized Picrosirius Med	Normalized Picrosirius Post	MRV Ant	MRV Med	MRV Post
169.9	167.6	100.0	100.0	100.0	0.3	0.3	0.3
54.5	48.6	45.7	32.1	29.0	0.2	0.2	0.2
78.3	74.3	47.9	46.1	44.4	0.4	0.5	0.4
71.9	55.1	44.5	42.3	32.9	0.3	0.5	0.4
104.1	85.3	82.9	61.3	50.9	0.2	0.3	0.3
95.1	86.7	70.7	56.0	51.7	0.5	0.6	0.4
108.0	107.8	69.9	63.5	64.3	0.4	0.5	0.5
88.2	78.1	63.9	51.9	46.6	0.2	0.3	0.3
130.2	124.4	79.9	76.7	74.3	0.4	0.5	0.4
123.6	126.1	85.1	72.8	75.2	0.3	0.4	0.4
141.5	111.9	103.1	83.3	66.8	0.2	0.4	0.3
122.6	133.8	77.9	72.2	79.8	0.4	0.5	0.4
130.2	119.5	87.3	76.7	71.3	0.4	0.5	0.4
78.9	64.1	50.8	46.4	38.2	0.1	0.3	0.2
67.6	59.9	42.2	39.8	35.8	0.3	0.4	0.3
50.2	60.9	43.1	29.6	36.4	0.2	0.3	0.3
80.6	84.3	59.8	47.4	50.3	0.2	0.4	0.2
63.1	67.6	52.6	37.1	40.4	0.4	0.5	0.3
73.0	88.2	53.3	43.0	52.6	0.4	0.4	0.2
92.4	86.6	60.9	54.4	51.7	0.2	0.2	0.3
109.5	96.7	81.0	64.5	57.7	0.3	0.5	0.3
119.5	106.8	83.6	70.3	63.8	0.4	0.5	0.4
88.2	77.1	47.4	51.9	46.0	0.1	0.2	0.3
84.1	78.3	59.2	49.5	46.8	0.3	0.4	0.4
64.4	65.5	37.1	37.9	39.1	0.3	0.4	0.4
112.2	76.0	75.3	66.1	45.4	0.2	0.2	0.3
146.6	148.7	91.8	86.3	88.7	0.4	0.5	0.4
143.9	133.3	94.9	84.7	79.6	0.3	0.5	0.4
55.5	45.2	47.3	32.7	27.0	0.2	0.2	0.2
43.3	49.4	38.0	25.5	29.5	0.3	0.3	0.3
36.0	40.5	26.7	21.2	24.2	0.3	0.4	0.4
54.1	54.5	42.8	31.9	32.5	0.2	0.2	0.2
52.8	57.8	37.2	31.1	34.5	0.3	0.3	0.3
57.8	51.9	40.4	34.0	31.0	0.3	0.4	0.2
80.3	77.5	68.2	47.3	46.2	0.4	0.5	0.3
76.8	54.7	53.9	45.2	32.6	0.2	0.3	0.2
60.1	46.1	44.5	35.4	27.5	0.1	0.2	0.2

has never been used as a decellularization agent; nonetheless, it is a potent detergent employed as preservative in many drugs, like glaucoma eye drops, which associates high levels of cytotoxicity.[25] Although previous works by different groups described the accuracy of nondetergent decellularization agents, such as sodium chloride,[10,12,26] decellularization of a complete animal cornea likely requires the use of more potent decellularization agents (i.e., the most frequently used ionic and nonionic detergents)

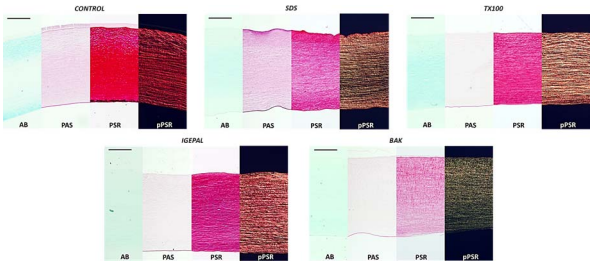

Figure 2. ECM components preservation of NPC and DPC subjected to the different decellularization protocols. Illustrative images correspond to samples decellularized for 48 hours using 0.1% concentrations of each agent. For each protocol, four images are shown corresponding to the immunohistochemical staining using alcian blue (AB), PAS, picrosirius red staining (PSR), and polarized picrosirius red staining (pPSR). *Scale bar*: 300 μm.

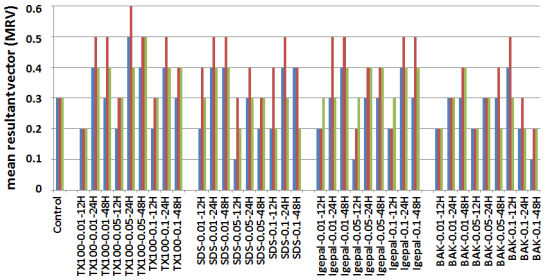

Figure 4. Analysis of collagen fibers orientation based on the evaluation of mean resultant vector (MRV) using the SurfCharJ ImageJ plug-in in NPC and DPC subjected to the different decellularization protocols. For each sample, the MRV is shown for the anterior (*blue*), medium (*red*), and posterior (*green*) areas of the cornea ($n = 3$).

despite the alterations that these agents could produce in the ECM. Future works should be carried out to determine the usefulness of other detergents such as Tween-20 or saponin in cornea decellularization.

First, our results revealed that most decellularization protocols were not able to remove a significant percentage of cells from the animal cornea. In contrast with previous works, the efficiency of cell elimination was very poor except for certain specific times and concentrations of SDS,[12,17–21] suggesting that 0.1% SDS for 48 hours could be efficiently used for whole-cornea decellularization. The low decellularization efficacy of the rest of protocols could be explained by the presence of the SCL surrounding the cornea. The circumferential fibers in the corneal periphery[27] together with other structures such as the Schlem's canal, the Vogt palisades and the epithelial crypts in the SCL could represent a rigid rim that act as a barrier against the deformation of the cornea by swelling. In addition, we found that the efficiency of most decellularization protocols was not time-dependent, suggesting that the type of agent and its concentration were the most important factors related to cell removal efficiency. Although previous reports found that time is an important factor for decellularization of other tissue types,[15] the presence of the SCL barrier on whole corneas may impair decellularization even for the highest incubation times. Therefore, decellularization of whole corneas may not be dependent on time, except for certain detergents previously known to have strong decellularization power such as SDS. As expected, the highest concentrations of SDS were associated to improved decellularization efficiencies, with a positive correlation with agent concentration.

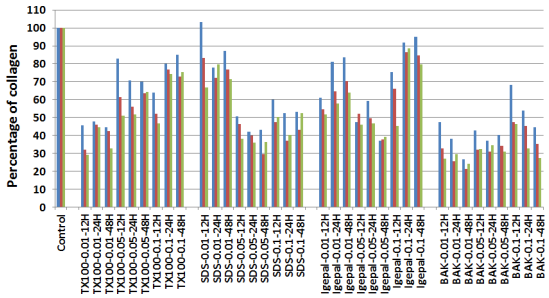

Figure 3. Collagen preservation as determined by PSR histochemical staining of NPC and DPC subjected to the different decellularization protocols. The percentage of remaining collagen fibers is shown for each group of samples and for the anterior (*blue*), medium (*red*), and posterior (*green*) areas of the cornea ($n = 3$) using NPC as control.

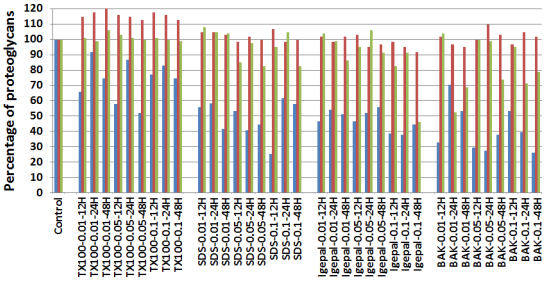

Figure 5. Proteoglycans preservation as determined by AB histochemical staining of NPC and DPC subjected to the different decellularization protocols. The percentage of remaining proteoglycans is shown for each group of samples and for the anterior (*blue*), medium (*red*), and posterior (*green*) areas of the cornea ($n = 3$) using NPC as control.

Once the animal corneas were decellularized, it is very important to verify that the histological structure of the decellularized tissues is preserved. Ideally, a decellularization agent should be able to eliminate all cells from the tissue while maintaining all the fibrillar and nonfibrillar components of the ECM.[15,28] In the case of the cornea, the major fibrillar component is type-I collagen, which should be preserved and properly oriented for a correct cornea function.[27,29,30] In this sense, our results showed that all protocols altered the collagen contents of the cornea, although the two agents with better results were Igepal followed by SDS, and these agents were able to preserve fiber orientation as compared with control corneas. These results are consistent with the idea that very powerful protocols are necessary for whole-cornea decellularization, and this could damage the ECM. Interestingly, the agent that more intensely damaged the collagen structure and alignment of the cornea was BAK, a component that is commonly present in pharmacological eye drops,[25] as we can see in the collagen staining and fiber orientation analysis.

Two of the most important nonfibrillar ECM components are proteoglycans and glycoproteins, which contribute to maintain the corneal lamellar pattern.[31–34] Proteoglycans and glycoproteins are located between collagen fibers leading to establish a well-defined distance between collagen fibers that generates the lamellar pattern.[29,31,35] Therefore, to preserve both kinds of molecules is necessary to maintain the normal structural characteristics of the native cornea. Regarding the proteoglycans, all decellularization protocols preserved high levels of these components; however, the concentration of glycoproteins was decreased after the decellularization process. Globally, the decellularization agent that most efficiently preserved both components was SDS, thus confirming the usefulness of this detergent for cornea decellularization.

Interestingly, our results revealed the existence of important differences among corneal regions in control undecellularized corneas. As shown in the results, control corneas showed a well-defined pattern in which an anterior, a medium, and a posterior region were identifiable in the stroma, suggesting that anatomical and histological differences exist among the stroma. This could explain our results showing important differences among the three areas of the cornea after being submitted to each decellularization protocol. The existence of different regions in the stroma could have important clinical implications and could help to understand why some corneal diseases only affect specific regions of the corneal stroma. The origin of these regionalized differences could be found in the development of the cornea in the embryo when the mesenchymal cells from the neural crest in a second wave penetrate between the primordium of the corneal epithelium and the corneal endothelium.[36] After some weeks, these mesenchymal cells concentrate underneath the corneal epithelium and over the endothelium,[37] where they could secrete high amounts of proteoglycans in the context of an epithelium-mesenchyme interaction like take place in the development of the tooth,[38] kidney,[39] and hair follicle.[40] Although these results need to be confirmed by additional studies, the fact that the anterior stroma region is very rich in cells and poor in glycosaminoglycans and collagen compactation may support the idea of using only the medium and posterior regions of the porcine cornea for decellularization purposes, since these regions demonstrated higher decellularization efficiency. In addition, the anterior region of the cornea showed a significant loss of proteoglycans after decellularization, whereas no differences with the control corneas were found for the medium and posterior cornea regions. However, the anterior region of the cornea showed the highest concentrations of glycoproteins after decellularization. Taken together, all these data suggest that the decellularization effects of the different agents used in this work differed among cornea regions, and this should be taken into account from a clinical standpoint.

All these results suggest that decellularization of whole corneas could be efficiently achieved in laboratory, although it is likely that new decellularization protocols based on the use of other detergents such as saponin or Tween-20,[41] or the combination of detergents with other decellularizing agents such as DNAse orRNAse[12,42] should be developed. In the future, decellularized whole corneas could represent a new alternative to corneal human donors in corneal transplants,[14] and these organs could have clinical usefulness for the treatment of patients with SCL damage. Furthermore, once we have demonstrated that whole-porcine corneas can be decellularized, future studies should determine the validness of these methods for decellularizing corneas obtained from other animals, or even from human origin. Previous reports suggest that animal corneas could trigger in vivo immune response leading to organ rejection, even though the cornea is considered to be immunepriviliged.[43] The immunogenicity of these decellularized porcine corneas should be determined in vivo to ensure long in vivo graft survival rates.[43] In addition,

Table 2. Quantitative Analysis of Proteoglycans Preservation as Determined by Alcian Blue Histochemical Staining and Glycoproteins Preservation as Determined by PAS Histochemical Staining

	Alcian Blue Ant	Alcian Blue Med	Alcian Blue Post	Normalized Alcian Blue Ant	Normalized Alcian Blue Med
Control NPC	13.5	6.1	8	100	100
TX100-0.01, 12 h	8.9	7	8.1	65.9	115
TX100-0.01, 24 h	12.4	7.2	7.9	91.9	118
TX100-0.01, 48 h	10.1	7.5	8.5	74.8	123
TX100-0.05, 12 h	7.8	7.1	8.2	57.8	116
TX100-0.05, 24 h	11.7	7	8.1	86.7	115
TX100-0.05, 48 h	7	6.9	8	51.9	113
TX100-0.1, 12 h	10.4	7.2	8.1	77	118
TX100-0.1, 24 h	11.2	7.1	8	83	116
TX100-0.1, 48 h	10.1	6.9	7.9	74.8	113
SDS-0.01, 12 h	7.5	6.4	8.6	55.6	105
SDS-0.01, 24 h	7.9	6.4	8.4	58.5	105
SDS-0.01, 48 h	5.6	6.3	8.3	41.5	103
SDS-0.05, 12 h	7.2	6	6.8	53.3	98.4
SDS-0.05, 24 h	5.5	6.2	7.8	40.7	102
SDS-0.05, 48 h	6	6.1	6.6	44.4	100
SDS-0.1, 12 h	3.4	6.5	7.6	25.2	107
SDS-0.1, 24 h	8.3	6	8.4	61.5	98.4
SDS-0.1, 48 h	7.8	6.1	6.6	57.8	100
Igepal-0.01, 12 h	6.3	6.2	8.3	46.7	102
Igepal-0.01, 24 h	7.3	6	7.9	54.1	98.4
Igepal-0.0, 48 h	6.9	6.2	6.9	51.1	102
Igepal-0.05, 12 h	6.3	6.3	7.6	46.7	103
Igepal-0.05, 24 h	7	5.8	8.5	51.9	95.1
Igepal-0.05, 48 h	7.5	5.9	7.3	55.6	96.7
Igepal-0.1, 12 h	5.2	6	6.6	38.5	98.4
Igepal-0.1, 24 h	5.1	5.8	7.3	37.8	95.1
Igepal-0.1, 48 h	6	5.6	3.7	44.4	91.8
BAK-0.01, 12 h	4.4	6.2	8.3	32.6	102
BAK-0.01, 24 h	9.5	5.9	4.2	70.4	96.7
BAK-0.01, 48 h	7.2	5.8	5.5	53.3	95.1
BAK-0.05, 12 h	4	6.1	8	29.6	100
BAK-0.05, 24 h	3.7	6.7	7.9	27.4	110
BAK-0.05, 48 h	5.1	6.3	5.9	37.8	103
BAK-0.1, 12 h	7.2	5.9	7.6	53.3	96.7
BAK-0.1, 24 h	5.3	6.4	5.7	39.3	105
BAK-0.1, 48 h	3.5	6.2	6.3	25.9	102

Average results are shown for each sample as raw values and normalized values after considering the results obtained for control NPC as 100%.

future works should determine the ability of DPC to support cell growth after decellularization.[42] If this is the case, DPC could be recellularized with human cornea cells, including limbal stem cells, thus allowing the generation of artificial whole corneas for clinical use. On the one hand, these corneas could eventually be used for the replacement of corneas with limbal failure by full-thickness keratoplasty. On the other hand, knowledge on the regional differences in decellularized corneas will allow us to select the more

Table 2. Extended.

Normalized Alcian Blue Post	PAS Ant	PAS Med	PAS Post	Normalized PAS Ant	Normalized PAS Med	Normalized PAS Post
100	18.3	24.6	21.3	100	100	100
101	14.1	10.7	8.5	76.8	43.7	39.9
98.8	15.8	13.7	10.7	86.1	55.6	50
106	13.6	11.1	10.6	74	45.2	49.6
103	14.5	13.1	10.5	79.2	53.4	49.4
101	16.2	12.7	10.9	88.7	51.6	51.2
100	14.6	12.2	11.6	79.9	49.7	54.6
101	12.7	11.4	8.6	69.1	46.2	40.4
100	8.9	10	10.3	48.7	40.6	48.3
98.8	11.1	10.3	10.8	60.7	41.9	50.6
108	19.1	16.9	12.3	105	68.6	57.8
105	18.4	14.6	13.1	100	59.3	61.3
104	17.8	16.5	16.5	97.2	67.2	77.5
85	13.8	11.3	8.3	75.3	46.1	38.9
97.5	12.5	11.6	10.9	68.5	47.2	51.3
82.5	12.4	9.6	9.4	67.8	38.9	44.2
95	14.6	10.4	9.3	79.5	42.5	43.9
105	12.7	10.1	9.5	69.4	41.2	44.8
82.5	13	10	9.6	71	40.7	45.1
104	17.3	14.1	14.6	94.4	57.4	68.4
98.8	17	15.4	12.1	92.7	62.5	56.8
86.3	15.9	12.9	12.5	86.7	52.5	58.8
95	14.6	15.7	10.7	80	63.8	50.1
106	14.3	13.2	12.6	78.2	53.8	59.2
91.3	12.8	11.9	12	70.1	48.4	56.5
82.5	18	18.3	11.9	98.2	74.5	55.9
91.3	18.3	17.5	12.2	100	71.1	57.3
46.3	15.7	14.2	13.5	85.9	57.6	63.2
104	18	18.1	15.4	98.4	73.4	72.2
52.5	18.6	14.7	14.6	102	59.8	68.5
68.8	15.8	12.9	13.5	86.5	52.4	63.2
100	12.1	10.6	8.1	66.2	43.2	37.9
98.8	10.8	10.4	9.9	59.2	42.2	46.5
73.8	13.1	10	9.8	71.4	40.6	46.2
95	13.5	11.4	10.2	73.7	46.4	47.6
71.3	13	10.8	10.8	71.1	44	50.5
78.8	11.3	9.5	7.5	61.9	38.7	35.1

appropriate regional model for the generation of lamelar corneas for clinical use, lamelar keratoplasty. Finally, the optical differences between the human and the porcine cornea warrant future studies focused on the optical behavior of DPC grafted in vivo.

In summary, SDS appears as one of the best detergents for decellularizing whole-porcine corneas. Therefore, SDS appears as one of the best protocols for decellularization of whole corneas including the SCL, not only due to its efficiency, especially on certain regions of the cornea, but also because it is easy-handle and straightforward. In

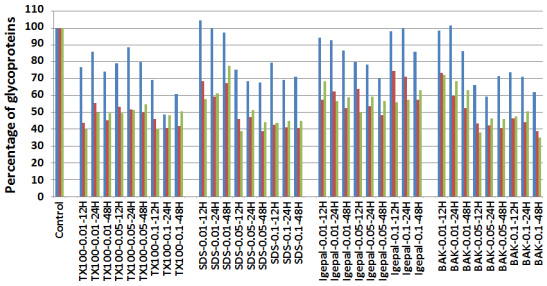

Figure 6. Glycoproteins preservation as determined by PAS histochemical staining of NPC and DPC subjected to the different decellularization protocols. The percentage of remaining glycoproteins is shown for each group of samples and for the anterior (*blue*), medium (*red*), and posterior (*green*) areas of the cornea ($n = 3$) using NPC as control.

vivo studies should establish the real translational potential of these decellularized organs.

Acknowledgments

Supported by grants from the Spanish Plan Nacional de Investigación Científica, Desarrollo e Innovación Tecnológica (I+D+I) from the Spanish Ministry of Economy and Competitiveness (Instituto de Salud Carlos III), Grants FIS PI11/2680 and FIS PI11/1582 (cofinanced by FEDER funds, European Union), and by Grants PI-0462-2010 and P10-CTS-6060 from Consejería de Igualdad, Salud y Políticas Sociales and Consejería de Economía, Innovación, Ciencia y Empleo, Junta de Andalucia, Spain.

Disclosure(s): **M González-Andrades,** None; **V. Carriel,** None; **M Rivera-Izquierdo,** None; **I Garzón,** None; **E. González-Andrades,** None; **S. Medialdea,** None; **M. Alaminos,** None; **A. Campos,** None

References

1. Schwartz EC, Huss R, Hopkins A, et al. Blindness and visual impairment in a region endemic for onchocerciasis in the Central African Republic. *Br J Ophthalmol*. 1997;81:443–447.
2. Whitcher JP, Srinivasan M, Upadhyay MP. Corneal blindness: a global perspective. *Bull World Health Organ*. 2001;79:214–221.
3. Oliva MS, Schottman T, Gulati M. Turning the tide of corneal blindness. *Indian J Ophthalmol*. 2012;60:423–427.
4. Alaminos M, Del Carmen Sanchez-Quevedo M, Munoz-Avila JI, et al. Construction of a complete rabbit cornea substitute using a fibrin-agarose scaffold. *Invest Ophthalmol Vis Sci*. 2006;47:3311–3317.
5. Gonzalez-Andrades M, Garzón I, Alaminos M, et al. Advances in the field of tissue engineering and regenerative medicine: state of the art and regulatory issues. *J Biomater Tissue Eng*. 2013;3:245–260.
6. Cardona Jde L, Ionescu AM, Gomez-Sotomayor R, et al. Transparency in a fibrin and fibrin-agarose corneal stroma substitute generated by tissue engineering. *Cornea*. 2011;30:1428–1435.
7. Gonzalez-Andrades M, Garzon I, Gascon MI, et al. Sequential development of intercellular junctions in bioengineered human corneas. *J Tissue Eng Regen Med* 2009;3:442–449.
8. Fagerholm P, Lagali NS, Ong JA, et al. Stable corneal regeneration four years after implantation of a cell-free recombinant human collagen scaffold. *Biomaterials*. 2014;35:2420–2427.
9. Lawrence BD, Marchant JK, Pindrus MA, Omenetto FG, Kaplan DL. Silk film biomaterials for cornea tissue engineering. *Biomaterials*. 2009;30:1299–1308.
10. Gonzalez-Andrades M, de la Cruz Cardona J, Ionescu AM, Campos A, Del Mar Perez M, Alaminos M. Generation of bioengineered corneas with decellularized xenografts and human keratocytes. *Invest Ophthalmol Vis Sci*. 2011;52:215–222.
11. Wilson SL, Sidney LE, Dunphy SE, Rose JB, Hopkinson A. Keeping an eye on decellularized corneas: a review of methods, characterization and applications. *J Funct Biomater*. 2013;4:114–161.
12. Shafiq MA, Gemeinhart RA, Yue BY, Djalilian AR. Decellularized human cornea for reconstructing the corneal epithelium and anterior stroma. *Tissue Eng Part C Methods*. 2012;18:340–348.
13. Oliveira AC, Garzon I, Ionescu AM, et al. Evaluation of small intestine grafts decellularization methods for corneal tissue engineering. *PLoS One*. 2013;8:e66538.
14. Lynch AP, Ahearne M. Strategies for developing decellularized corneal scaffolds. *Exp Eye Res*. 2013;108:42–47.
15. Crapo PM, Gilbert TW, Badylak SF. An overview of tissue and whole organ decellularization processes. *Biomaterials*. 2011;32:3233–3243.
16. Badylak SF, Taylor D, Uygun K. Whole-organ tissue engineering: decellularization and recellularization of three-dimensional matrix scaffolds. *Annu Rev Biomed Eng*. 2011;13:27–53.

17. Fan XQ, Chen P, Fu Y. Xenogenic corneal acellular matrix as carrier for reconstruction of biological cornea epithelium-scaffold-endothelium compound [in Chinese]. *Zhonghua Yan Ke Za Zhi* 2007;43:437–441.
18. Fang XF, Zhao J, Shi WY, Xie LX. Biocompatibility of acellular corneal stroma and transplantation of tissue-engineered corneal epithelium [in Chinese]. *Zhonghua Yan Ke Za Zhi*. 2008;44:934–942.
19. Sasaki S, Funamoto S, Hashimoto Y, et al. In vivo evaluation of a novel scaffold for artificial corneas prepared by using ultrahigh hydrostatic pressure to decellularize porcine corneas. *Mol Vis*. 2009;15:2022–2028.
20. Fu Y, Fan X, Chen P, Shao C, Lu W. Reconstruction of a tissue-engineered cornea with porcine corneal acellular matrix as the scaffold. *Cells Tissues Organs*. 2010;191:193–202.
21. Pang K, Du L, Wu X. A rabbit anterior cornea replacement derived from acellular porcine cornea matrix, epithelial cells and keratocytes. *Biomaterials*. 2010;31:7257–7265.
22. Kasimir MT, Rieder E, Seebacher G, Wolner E, Weigel G, P. Simon Presence and elimination of the xenoantigen gal (alpha1, 3) gal in tissue-engineered heart valves. *Tissue Eng*. 2005;11:1274–1280.
23. Neethling WM, Yadav S, Hodge AJ, Glancy R. Enhanced biostability and biocompatibility of decellularized bovine pericardium, crosslinked with an ultra-low concentration monomeric aldehyde and treated with ADAPT. *J Heart Valve Dis*. 2008;17:456–463, discussion 464.
24. Mangold S, Schrammel S, Huber G, et al. Evaluation of decellularized human umbilical vein (HUV) for vascular tissue engineering - comparison with endothelium-denuded HUV. *J Tissue Eng Regen Med*. 2015;9:13–23.
25. Noecker R, Miller KV. Benzalkonium chloride in glaucoma medications. *Ocul Surf*. 2011;9:159–162.
26. Oh JY, Kim MK, Lee HJ, Ko JH, Wee WR, Lee JH. Processing porcine cornea for biomedical applications. *Tissue Eng Part C Methods* 2009;15:635–645.
27. Kamma-Lorger CS, Boote C, Hayes S, et al. Collagen and mature elastic fibre organisation as a function of depth in the human cornea and limbus. *J Struct Biol*. 2010;169:424–430.
28. Gilbert TW, Sellaro TL, Badylak SF. Decellularization of tissues and organs. *Biomaterials*. 2006;27:3675–3683.
29. Meek KM, Leonard DW, Connon CJ, Dennis S, Khan S. Transparency, swelling and scarring in the corneal stroma. *Eye*. 2003;17:927–936.
30. Meek KM, Fullwood NJ. Corneal and scleral collagens–a microscopist's perspective. *Micron*. 2001;32:261–272.
31. Quantock AJ, Young RD. Development of the corneal stroma, and the collagen-proteoglycan associations that help define its structure and function. *Dev Dyn*. 2008;237:2607–2621.
32. Ren R, Hutcheon AE, Guo XQ, et al. Human primary corneal fibroblasts synthesize and deposit proteoglycans in long-term 3-D cultures. *Dev Dyn*. 2008;237:2705–2715.
33. Schlotzer-Schrehardt U, Dietrich T, Saito K, et al. Characterization of extracellular matrix components in the limbal epithelial stem cell compartment. *Exp Eye Res*. 2007;85:845–860.
34. Funderburgh JL. Keratan sulfate: structure, biosynthesis, and function. *Glycobiology*. 2000;10:951–958.
35. Hassell JR, Birk DE. The molecular basis of corneal transparency. *Exp Eye Res*. 2010;91:326–335.
36. Zieske JD. Corneal development associated with eyelid opening. *Int J Dev Biol*. 2004;48:903–911.
37. Sevel D, Isaacs R. A re-evaluation of corneal development. *Trans Am Ophthalmol Soc*. 1988;86:178–207.
38. Thesleff I, Jalkanen M, Vainio S, Bernfield M. Cell surface proteoglycan expression correlates with epithelial-mesenchymal interaction during tooth morphogenesis. *Dev Biol*. 1988;129:565–572.
39. Ekblom P. Formation of basement membranes in the embryonic kidney: an immunohistological study. *J Cell Biol*. 1981;91:1–10.
40. Kishimoto J, Ehama R, Wu L, Jiang S, Jiang N, Burgeson RE. Selective activation of the versican promoter by epithelial- mesenchymal interactions during hair follicle development. *Proc Natl Acad Sci U S A*. 1999;96:7336–7341.
41. Booth C, Korossis SA, Wilcox HE, et al. Tissue engineering of cardiac valve prostheses I: development and histological characterization of an acellular porcine scaffold. *J Heart Valve Dis*. 2002;11:457–462.
42. Yoeruek E, Bayyoud T, Maurus C, et al. Decellularization of porcine corneas and repopulation with human corneal cells for tissue-engineered xenografts. *Acta Ophthalmol*. 2012;90:e125–e131.
43. Niederkorn JY. The immune privilege of corneal allografts. *Transplantation*. 1999;67:1503–1508.